Sustainable hydrogen production from seawater and sewage treated water using reverse electrodialysis technology

Mitsuru Higa **IWA**[a,*], Takeshi Watanabe[b], Masahiro Yasukawa[a], Nobutaka Endo[a], Yuriko Kakihana[a], Hidenobu Futamura[b], Katsuhiro Inoue[b], Haruo Miyake[c], Jiro Usui[c], Azusa Hayashi[c] and Manabu Matsuhashi[d]

[a] Yamaguchi University, 2-16-1 Tokiwadai, Ube, Yamaguchi 755-8611, Japan

[b] Seiko Electric Co., Ltd., 7-25 2-Chome Hakata-ku, Fukuoka City 812-0008, Japan

[c] Japan Sewage Works Agency, 2-31-27 Yushima, Bunkyo-ku, Tokyo 113-0034, Japan

[d] National Institute for Land and Infrastructure Management, 1 Asahi, Tsukuba City, Ibaraki, Japan

*Corresponding author. E-mail: mhiga@yamaguchi-u.ac.jp

Abstract

A pilot-scale sustainable hydrogen production system using reverse electrodialysis (RED) technology was launched. The system is based on direct conversion of salinity gradient energy (SGE) between seawater (SW) and sewage treated water (STW) to hydrogen production by water electrolysis. The hydrogen production rate was almost the same as the theoretical value. This indicates that the RED hydrogen production system can convert SGE between SW and STW to hydrogen energy at high current efficiency.

Key words: hydrogen production, reverse electrodialysis, salinity gradient energy

INTRODUCTION

Utilization of renewable energy and its diversification is quite important to ensure energy safety for human's sustainability. Since renewable energy such as solar- and wind-based energy has intermittent and fluctuating characteristics, power-to-gas technology has a great interest to control electricity grid by utilizing electricity to split water into hydrogen (H_2) and oxygen (O_2) (Götz et al. 2016). This H_2 can be used as efficient gaseous fuel for fuel cell vehicle (Mori & Hirose 2009), fuel cell-based power supplying system (Reiter & Lindorfer 2015), injection into a natural gas pipeline network (Walker et al. 2016) and hydrogen-fueled combustion turbine for electric power generation (Taamallah et al. 2015) without CO_2 emission. Therefore, to overcome the intermittent and fluctuating nature of renewable energy, a combination of renewable energy-based electricity and hydrogen are promising to be useful in future.

Salinity gradient energy (SGE) is a sustainable and environmentally friendly energy related to the electrochemical potential between two solutions with different salinities (Giacalone et al. 2018). It has been theoretically estimated that about 0.5 kWh of energy can be potentially captured by mixing 1 m³ of seawater (SW) with 1 m³ of river water (Veerman et al. 2009), and the estimated global potential is 2,000 TWh/year (Logan & Elimelech 2012). Because Japan is an island nation, there are many opportunities to access fresh water and SW simultaneously along the coastline, such as various manufacturing factories, thermal power plants, municipal wastewater plants and

so on, where fresh wastewater is discharged into the sea directly after adequate treatment. Therefore, SGE between these fresh water and SW streams potentially can be utilized.

Reverse electrodialysis (RED) is one of the emerging technologies for capturing SGE by applying ion exchange membranes (IEMs) (Daniilidis *et al.* 2014; Hong *et al.* 2015). In RED, low salinity (LS) and high salinity (HS) solutions flow alternatively between anion-exchange membranes (AEMs) and cation-exchange membranes (CEMs). Anions and cations in the HS solution move to the LS solution through AEMs and CEMs in opposite directions under their respective concentration gradients, which can be converted to electricity by redox reaction on the electrodes (Holladay *et al.* 2009; Geise *et al.* 2013; Tedesco *et al.* 2015). If the optimum electrode and electrode solution is chosen, H_2 and O_2 are generated through water electrolysis reaction. Therefore, the RED system enables to directly convert SGE into useful gaseous fuels.

In this study, we demonstrate a direct hydrogen production system from SGE using RED technology, here called a RED-H_2 system, using SW and sewage treated water (STW). In Japan, about 17% of the sewage treatment plants directly dispose their treated wastewater into the sea, and therefore, there is a nice opportunity to generate H_2 (also O_2) using the system. Moreover, wastewater treatment plants exist in all communities and are often located in cities, which have a high H_2 demand, or their environs. This means that excess H_2 transportation is not needed and the RED-H_2 system can be easily used through a pipeline network in the respective local communities. Therefore, a RED-H_2 system in a sewage treatment plant near the sea will contribute to constructing decentralized energy systems with high social energy security and diversity in the future.

Figure 1 shows a schematic illustration of the RED-H_2 system. The system has number of pairs of energy converting cells stacked between two electrode compartments. Each cell has a CEM, an AEM and two flow channels of SW and STW, and will generate ca. 0.15 V when SW and STW are fed to the channels. Hence, for an example, the stack of 20 pairs of the cells will give ca. 3 V of voltage between the electrodes. Hydrogen and oxygen gases generate at the electrodes by water electrolysis driven by the voltage.
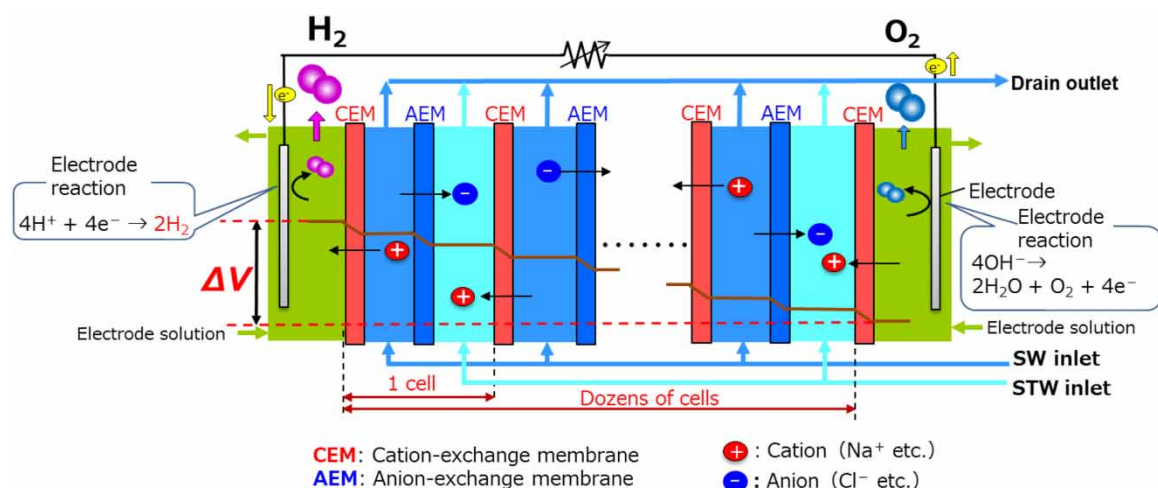
Figure 1 | A schematic diagram of a RED hydrogen production system.

MATERIAL AND METHODS

Figure 2 shows the flow chart of the RED-H_2 system built in Fukuoka city. In the system, Neosepta® AMX and CMX (Astom Co. Japan) were used as AEM and CEM, respectively. The fundamental properties of the membranes are listed in Table 1. These membranes are standard IEMs for electrodialysis
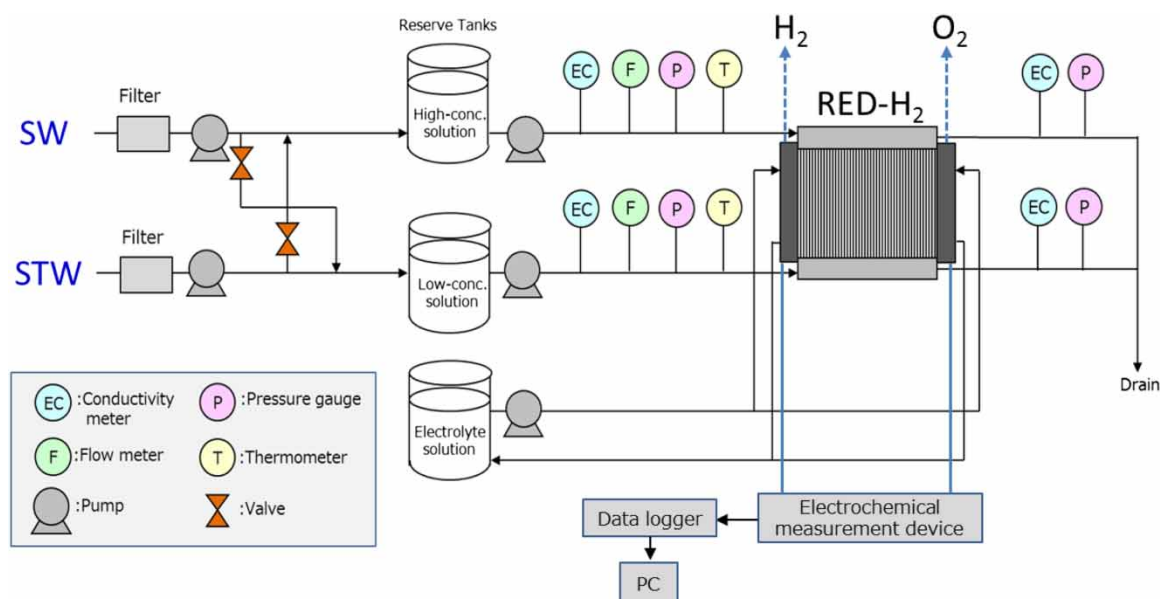
Figure 2 | A flow chart of the RED-H$_2$ system.

Table 1 | Fundamental properties of the membranes used in the RED-H$_2$ stack

Membrane	Thickness [μm]	Electric resistance [Ωcm^2]	Transport number [–]	Water content [–]
Neosepta® CMX	170–190	2.3	0.98<	0.25–0.30
Neosepta® AMX	160–180	3.0	0.98<	0.25–0.30

(ED) applications. In this study, a commercial ED stack was used as a RED-H$_2$ stack. The characteristics of the stack are listed in Table 2. The inter-membrane distance between CEM and AEM in the cell is 600 μm. The effective membrane area is 1,000 cm^2 (20 cm × 50 cm), and number of pairs of the cell was 200. Hence, the total membrane area of the stack was 40 m^2. The electrode material of the two electrodes was Pt coated titanium plates, and 5 wt% Na$_2$SO$_4$ was fed to the electrode compartments as electrode solutions. The electrodes were connected to an electrochemical measuring device (PLZ 164 W/Kikusui Electronics Co.) to change the load resistance for controlling the voltage-current relationship of the system. Generated H$_2$ and O$_2$ gases at the respective electrode were trapped using gas trapping instruments to measure the volume at a predetermined time interval.

Table 2 | Characteristics of RED-H$_2$ stack

Membranes	CMX/AMX
Active membrane area	0.1 m^2
Inter-membrane distance	600 μm
No. of pair	200
Total membrane area	40 m^2
Electrodes	Ti-Pt coating
Electrode solution	5 wt.% Na$_2$SO$_4$

STW was obtained from Wagiro water treatment center (Fukuoka, Japan). It was difficult for us to get SW directly from Hakata bay. Hence, brine from a SW desalination center (Fukuoka, Japan) with ca. 90 mS/cm of ionic conductivity and STW were mixed to get salt water with 50 mS/cm of ionic

conductivity, which is the same concentration as SW at Hakata bay. Here, the salt solution is called SW. Both the brine and STW were filtered by cartridge filter and fiber filter (pore size: 10 μm), respectively, and adequately mixed to control their ionic conductivity. After this, they were fed to RED-H$_2$ stack. Because the brine was already treated by sand filtration in the desalination plant, we chose cartridge filter for the brine. The STW was mainly treated by anaerobic-oxix activated sludge (A/O) process in Wagiro water treatment center. Ionic conductivity, hydraulic pressure, flow rate and temperature of SW and STW were monitored with measurement instruments at the indicated points in Figure 2. The experiment conditions in the test were listed in Table 3.

Table 3 | Experiment conditions of the RED-H$_2$ system

|	
Brine conductivity	78–96 mS/cm
SW conductivity	50 mS/cm
STW conductivity	1.0–2.5 mS/cm
SW flow rate	2–8 L/min
STW flow rate	2–8 L/min
Electric current	0.5–3.0 A
Water temperature	18–28.5 °C

RESULTS AND DISCUSSION

In an RED stack, theoretical maximum voltage (open circuit voltage: V_{OC}) is given in terms of the following equation (Mei & Tang 2018):

$$V_{OC} = \frac{2(t_+ + t_-)NRT}{F} \ln\left(\frac{\gamma_{HS}C_{HS}}{\gamma_{LS}C_{LS}}\right) \tag{1}$$

where F, R, z and T are Faraday constant, gas constant, valance of ions and temperature, respectively. t_+ and t_- are transport number of CEM and AEM, respectively. γ, x and C are activity coefficient, molar fraction of salt and salt concentration, respectively.

Theoretical V_{OC} under the experimental conditions is about 35.4 volt under an approximation that ion conductivity was converted into NaCl concentration. Figure 3 shows an example of the
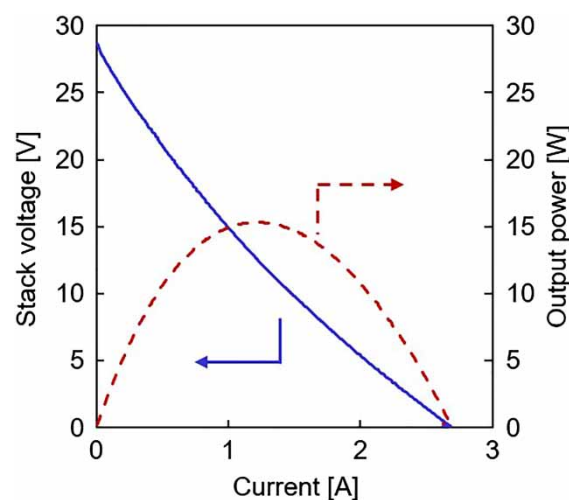
Figure 3 | The voltage and output power of the stack as a function of electric current. Solid curve: stack voltage; broken curve, output power. Flow rate of SW and STW was 4.3 L/min., water temperature, 28.5 °C.

voltage-current curve during the RED test. The open circuit voltage (current $= 0$) of the system showed 28.6 V, meaning that the stack voltage was about 20% less than the theoretical voltage. There will be two factors which cause VOC reduction: (1) the effect of divalent ions in SW such as Mg^{2+}, Ca^{2+} and SO_4^{2-} (Post *et al.* 2009), and (2) the decrease in the concentration ratio inside the stack even at zero current condition. The voltage decreased with increasing current, and the slope of the voltage-current curve then gives the internal electric resistance of the RED-H_2 stack. Theoretical internal electric resistance of the stack is given in terms of the following equations (Długołęcki *et al.* 2009).

$$R_{int} = R_{el} + N(R_{AEM} + R_{CEM} + R_{HS} + R_{LS})$$
$$= \frac{R_{el,m^2}}{S_m} + N\left(\frac{R_{AEM,m^2}}{S_m} + \frac{R_{CEM,m^2}}{S_m} + \frac{d_{HS}}{EC_{HS}S_m} + \frac{d_{LS}}{EC_{LS}S_m}\right) \quad (2)$$

where R, N, S_m, d and EC are resistance, number of cell pair, effective area, inter-membrane distance between CEM and AEM, and electric conductivity of the solutions, respectively. The subscripts of el, AEM, CEM, HS and LS are electrode, AEM, CEM, HS compartment and LS compartment, respectively. Subscript of m^2 means resistance per 1 m^2. Theoretical calculated resistance without electrode from salt concentrations of SW and STW at the inlet was 13.3 Ω, which was higher than the evaluated resistance (10 Ω) from the experimental data. In R_{int}, the R_{LS} is dominant (about 90% of R_{int} without R_{el}), and the R_{LS} decreased within the stack because electric conductivity of LS solution increased due to the salt diffusion from HS to LS along the current. Therefore, the R_{int} was slightly decreased with increasing the current. The output power became maximum of 15.3 W at 1.4 A of the current.

Figure 4 shows hydrogen production of the system at a constant current operation of 1.5 A as a function of time. The hydrogen production was directly proportional to the electric quantity (electric current $\times$ time). The hydrogen production rate calculated from the slope was 0.90 L/h, which is almost the same as the theoretical value. This indicates that the electric current conversion efficiency of hydrogen production in the system is ca. 100%.
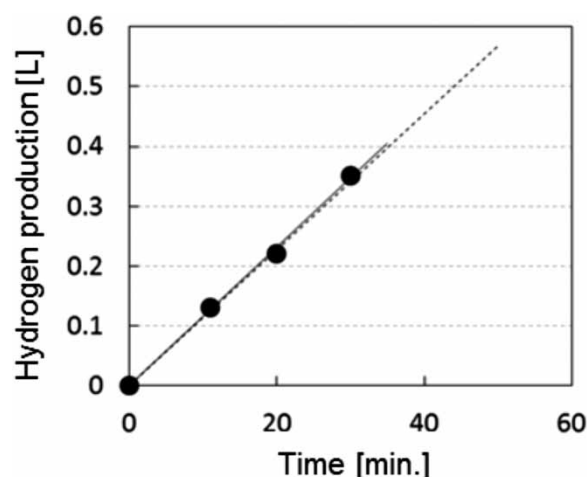

Figure 4 | Hydrogen production of the system as a function of time. Solid circles experiments; broken line, theoretical value obtained from the electric quantity. Flow rate of SW and STW was 4.3 L/min., water temperature, 28.5 °C.

Figure 5 shows the seasonal effect on water temperature and subsequent power output performance of the RED-H_2 system. During 7 months (Sep. 2016–Feb 2017), water temperature decreased from 28 °C to 18 °C, and about 30% of the power output decreased in this period. Because water temperature influences both V_{OC} and R_{int}, a higher temperature is suitable to obtain a higher energy output. From this evaluation, temperature dependence was estimated as about 3%/°C.
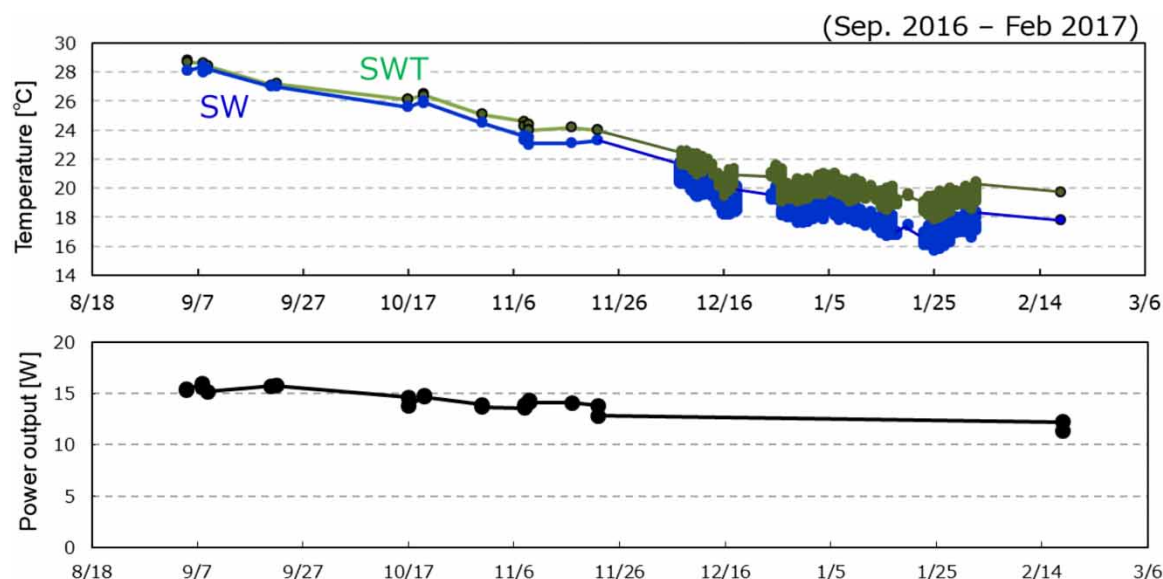
Figure 5 | Water temperature (SW and SWT) and power output performance during 7 months. Hydrogen production of the system as a function of time. Solid circles experiments; broken line, theoretical value obtained from the electric quantity. Flow rate of SW and STW was 4.3 L/min., water temperature, 28.5 °C. Flow rate of SW and STW was 4.3 L/min.

To estimate the possibility of long-time operation without pre-filtration, the long-time performance of the system without fiber filtration was evaluated. The converted power output (at 23 °C from the 3%/°C relation) is shown in Figure 6. We evaluated the converted power output without fiber filter by using STW directly. In this case, reduction of power output was not observed in 300 h even in the absence of fiber filter. However, after then, power output gradually decreased, and 80% reduction was observed at 800 h. The visual observation inside the stack after disassembling the stack revealed that this performance reduction would be caused by clogging of the foulants especially at the STW compartment. To investigate the performance recovery, we measured the performance after simple cleaning (without chemical treatment) inside of the disassembled stack. The converted power output of the system after cleaning was also shown in Figure 6. The result revealed that the simple cleaning allowed the power output performance (voltage and current) completely recovered. More-over, we also confirmed the resistance and thickness of the IEMs were same to those of initial values. Therefore, this results clearly supported the clogging of the foulants which was easy removable by simple cleaning was the main reason of performance reduction, and the membrane fouling was not severe (at least reversible). In addition, optimum method for cleaning in place (i.e. cleaning inside of
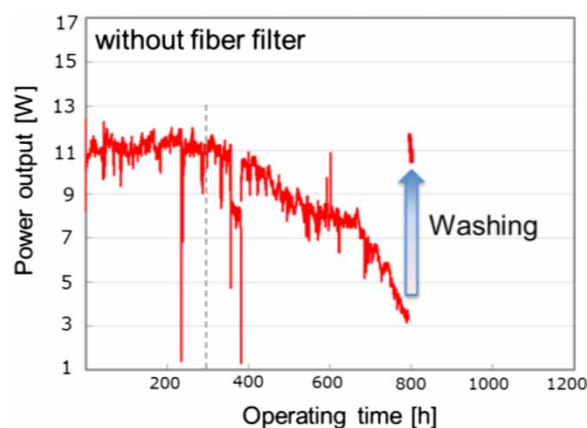
Figure 6 | Power output (converted to those at 23 °C) in long time operation without fiber filtration for STW. Flow rate of SW and STW was 4.3 L/min.

the RED-H_2 stack without disassembly) also should be developed in the future, to achieve stable H_2 (and O_2) production by utilizing this power output directly in water electrolysis.

CONCLUSIONS

In this research, we have developed the direct H_2 production system from SGE utilizing RED technology, called the RED-H_2 system, at pilot-scale. The RED-H_2 system can convert SGE between SW and STW to hydrogen at high current efficiency. Long-time evaluation of the RED-H_2 system revealed that temperature dependence of the performance was about 3%/°C, and stable operation in 1,100 h was achieved by using STW treated by fiber filtration (pore size: 10 μm). Because Japan has many opportunities, with 17% of sewage treatment plants directly disposing STW into the sea, the RED-H_2 system will contribute to developing a H_2 decentralized energy system network for high energy security and diversity in the future.

ACKNOWLEDGEMENTS

REFERENCES

Daniilidis, A., Vermaas, D. A., Herber, R. & Nijmeijer, K. 2014 Experimentally obtainable energy from mixing river water, seawater or brines with reverse electrodialysis. *Renewable Energy* **64**, 123–131.

Długołęcki, P., Gambier, A., Nijmeijer, K. & Wessling, M. 2009 Practical potential of reverse electrodialysis as process for sustainable energy generation. *Environmental Science & Technology* **43**, 6888–6894.

Geise, G. M., Curtis, A. J., Hatzell, M. C., Hickner, M. A. & Logan, B. E. 2013 Salt concentration differences alter membrane resistance in reverse electrodialysis stacks. *Environmental Science & Technology Letters* **1**(1), 36–39.

Giacalone, F., Catrini, P., Tamburini, A., Cipollina, A., Piacentino, A. & Micale, G. 2018 Exergy analysis of reverse electrodialysis. *Energy Conversion and Management* **164**, 588–602.

Götz, M., Lefebvre, J., Mörs, F., Koch, A. M., Graf, F., Bajohr, S., Reimert, R. & Kolb, T. 2016 Renewable Power-to-Gas: a technological and economic review. *Renewable Energy* **85**, 1371–1390.

Holladay, J. D., Hu, J., King, D. L. & Wang, Y. 2009 An overview of hydrogen production technologies. *Catalysis Today* **139**, 244–260.

Hong, J. G., Zhang, B., Glabman, S., Uzal, N., Dou, X., Zhang, H., Wei, X. & Chen, Y. 2015 Potential ion exchange membranes and system performance in reverse electrodialysis for power generation: a review. *Journal of Membrane Science* **486**, 71–88.

Logan, B. E. & Elimelech, M. 2012 Membrane-based processes for sustainable power generation using water. *Nature* **488**, 313–319.

Mei, Y. & Tang, C. Y. 2018 Recent developments and future perspectives of reverse electrodialysis technology: a review. *Desalination* **425**, 156–174.

Mori, D. & Hirose, K. 2009 Recent challenges of hydrogen storage technologies for fuel cell vehicles. *International Journal of Hydrogen Energy* **34**, 4569–4574.

Post, J. W., Hamelers, H. V. M. & Buisman, C. J. N. 2009 Influence of multivalent ions on power production from mixing salt and fresh water with a reverseelectro-dialysis system. *Journal of Membrane Science* **330**, 65–72.

Reiter, G. & Lindorfer, J. 2015 Global warming potential of hydrogen and methane production from renewable electricity via power-to-gas technology. *The International Journal of Life Cycle Assessment* **20**(4), 477–489.

Taamallah, S., Vogiatzaki, K., Alzahrani, F. M., Mokheimer, E. M. A., Habib, M. A. & Ghoniem, A. F. 2015 Fuel flexibility, stability and emissions in premixed hydrogen-rich gas turbine combustion: technology, fundamentals, and numerical simulations. *Applied Energy* **154**, 1020–1047.

Tedesco, M., Brauns, E., Cipollina, A., Micale, G., Modica, P., Russo, G. & Helsen, J. 2015 Reverse electrodialysis with saline waters and concentrated brines: a laboratory investigation towards technology scale-up. *Journal of Membrane Science* **492**, 9–20.

Veerman, J., Saakes, M., Metz, S. J. & Harmsen, G. J. 2009 Reverse electrodialysis: performance of a stack with 50 cells on the mixing of sea and river water. *Journal of Membrane Science* **327**(1–2), 136–144.

Walker, S. B., Mukherjee, U., Fowler, M. & Elkamel, A. 2016 Benchmarking and selection of Power-to-Gas utilizing electrolytic hydrogen as an energy storage alternative. *International Journal of Hydrogen* **41**, 7717–7731.